ELSEVIER

Native mass spectrometry-directed drug discovery: Recent advances in investigating protein function and modulation

KEYNOTE (GREEN)

Francesco Fiorentino [1,*], Dante Rotili [1,*], Antonello Mai [1,2]

[1] Department of Drug Chemistry and Technologies, Sapienza University of Rome, Piazzale Aldo Moro 5, 00185 Rome, Italy
[2] Pasteur Institute, Cenci-Bolognetti Foundation, Sapienza University of Rome, Piazzale Aldo Moro 5, 00185 Rome, Italy

Native mass spectrometry (nMS) is a biophysical method for studying protein complexes and can provide insights into subunit stoichiometry and composition, protein–ligand, and protein–protein interactions (PPIs). These analyses are made possible by preserving non-covalent interactions in the gas phase, thereby allowing the analysis of proteins in their native state. Consequently, nMS has been increasingly applied in early drug discovery campaigns for the characterization of protein–drug interactions and the evaluation of PPI modulators. Here, we discuss recent developments in nMS-directed drug discovery and provide a timely perspective on the possible applications of this technology in drug discovery.

Keywords: native mass spectrometry; protein–ligand interactions; protein–protein interactions; PROTAC; membrane proteins

Introduction

Proteins are a fundamental part of living organisms, given their involvement in all cellular pathways. They control all aspects of life, including, but not limited to, regulation of gene expression, catalysis of biochemical reactions, signaling, and transportation of molecules essential for cellular metabolism.[1] Therefore, non-covalent interactions between proteins and their partners (including other proteins, nucleic acids, lipids, carbohydrates, and small molecules) are at the core of myriad biological processes, such as transcriptional regulation, cell differentiation, immune response, cell adhesion, and inflammation. These interactions are governed by a variety of forces, including hydrogen bonds, electrostatic interactions, Van der Waals, and hydrophobic forces.[2] Importantly, the characterization of protein–ligand interactions is at the core of the drug discovery process. In fact, elucidation of protein structures and dynamics and the quantification of the kinetic and thermodynamic

Francesco Fiorentino graduated in medicinal chemistry from Sapienza University of Rome in 2016. He received his PhD in biophysical chemistry from the University of Oxford in 2020 under the supervision of Dame Carol Robinson, working on the elucidation of the structure and regulation of membrane proteins using mass spectrometry. Following a 1-year postdoc in the same lab, he joined the Mai group at Sapienza University of Rome as a postdoctoral researcher. His research focuses on the application of native mass spectrometry and other biophysical techniques to investigate the protein complexes involved in the epigenetic regulation of cellular homeostasis and in bacterial membrane biogenesis.

Dante Rotili graduated in medicinal chemistry from Sapienza University of Rome in 2003. He received his PhD in pharmaceutical sciences from the same University in 2007. From 2009 to 2010, he was a research associate in the Department of Chemistry, University of Oxford, where he worked in collaboration with Chris Schofield in the development of chemoproteomic probes for the characterization of 2-oxoglutarate-dependent enzymes. In 2020, he was appointed an associate professor of medicinal chemistry at Sapienza University of Rome. His research focuses mainly on the development of modulators of epigenetic enzymes with potential applications in cancer, neurodegenerative, metabolic, and infectious diseases.

Antonello Mai graduated in pharmacy from Sapienza University of Rome in 1984, from where he received his PhD in 1992 in pharmaceutical sciences under the supervision of M. Artico. In 1998, he was appointed associate professor of medicinal chemistry and, in 2011, full professor of medicinal chemistry at Sapienza University of Rome. His research interests include the synthesis and biological evaluation of new bioactive small-molecule compounds, in particular modulators of epigenetic targets, for use as chemotherapeutic agents against cancer, metabolic disorders, neurodegenerative diseases, and parasitic infections. In addition, he works in the fields of antibacterial/antimycobacterial, antiviral, and central nervous system agents.

* *Corresponding authors: Fiorentino, F. (f.fiorentino@uniroma1.it), Rotili, D. (dante.rotili@uniroma1.it).*

1359-6446/
https://doi.org/10.1016/j.drudis.2023.103548

parameters of protein–ligand binding constitute the earliest steps in the development of drugs that could be used to treat various pathologies.[3]

To date, a large toolbox of biophysical technologies is used during preclinical drug development to characterize protein–ligand interactions *in vitro*, each with its own set of strengths and shortcomings. These include isothermal titration calorimetry (ITC),[4] surface plasmon resonance (SPR),[5] nuclear magnetic resonance (NMR) spectroscopy,[6] and X-ray crystallography.[7] Despite the tremendous advances obtained by using these techniques, significant technological problems in drug development persist. Indeed, some protein species, such as dynamic protein oligomers and membrane protein complexes, remain difficult to target despite their enormous therapeutic potential. The transient nature of certain protein complexes, the instability of membrane proteins, and the possible lack of any enzymatic activity make these targets extremely challenging to investigate for drug development. Compounds that influence the function of these complicated targets cannot be easily evaluated by typical biophysical methods, which provide information on the average solution properties of the system and might not inform on single binding events or ligand influence on oligomeric states. Moreover, these approaches often require protein labeling or immobilization, which may alter the subtle equilibria being evaluated. Hence, complementary methodologies that increase our understanding of structural, thermodynamic, and kinetic features of drug action could accelerate preclinical drug development.

nMS is a promising methodology to investigate protein–ligand interactions that also allows the assessment of more challenging targets. It is a technique that enables the preservation of non-covalent interactions and quaternary protein structure in the gas phase. Moreover, unlike conventional denaturing MS, which often includes organic solvents and a low pH, nMS uses volatile, aqueous buffers at near-physiological pH and gentler voltages and ion transfer tube temperatures (usually <200 °C) compared with classic MS techniques. These differences with respect to other MS approaches contribute to the preservation of the native or native-like structures of the studied protein complexes.[8] This enables the quantification of dissociation constants for PPIs and protein–ligand interactions, the assessment of small-molecule mode of action, and the study of protein complex stoichiometry and subunit architecture and dynamics (Figure 1).[9]

nMS takes advantage of the milder nature of electrospray ionization (ESI) compared with other ionization methods [e.g., matrix-assisted laser desorption/ionization (MALDI), atmospheric pressure chemical ionization (APCI), or electron ionization (EI)] to transfer protein complexes from volatile buffered aqueous solutions into the gas phase and maintain the non-covalent interactions during this process.[10–12] The most common ionization method used in nMS is nanoESI (nESI), a subtype of ESI characterized by a smaller diameter of the capillary needle (usually 1–5 μm in nESI, whereas it reaches up to 0.5 mm in ESI) orifice and very slow flow rates (10–50 nl/min),[13] which

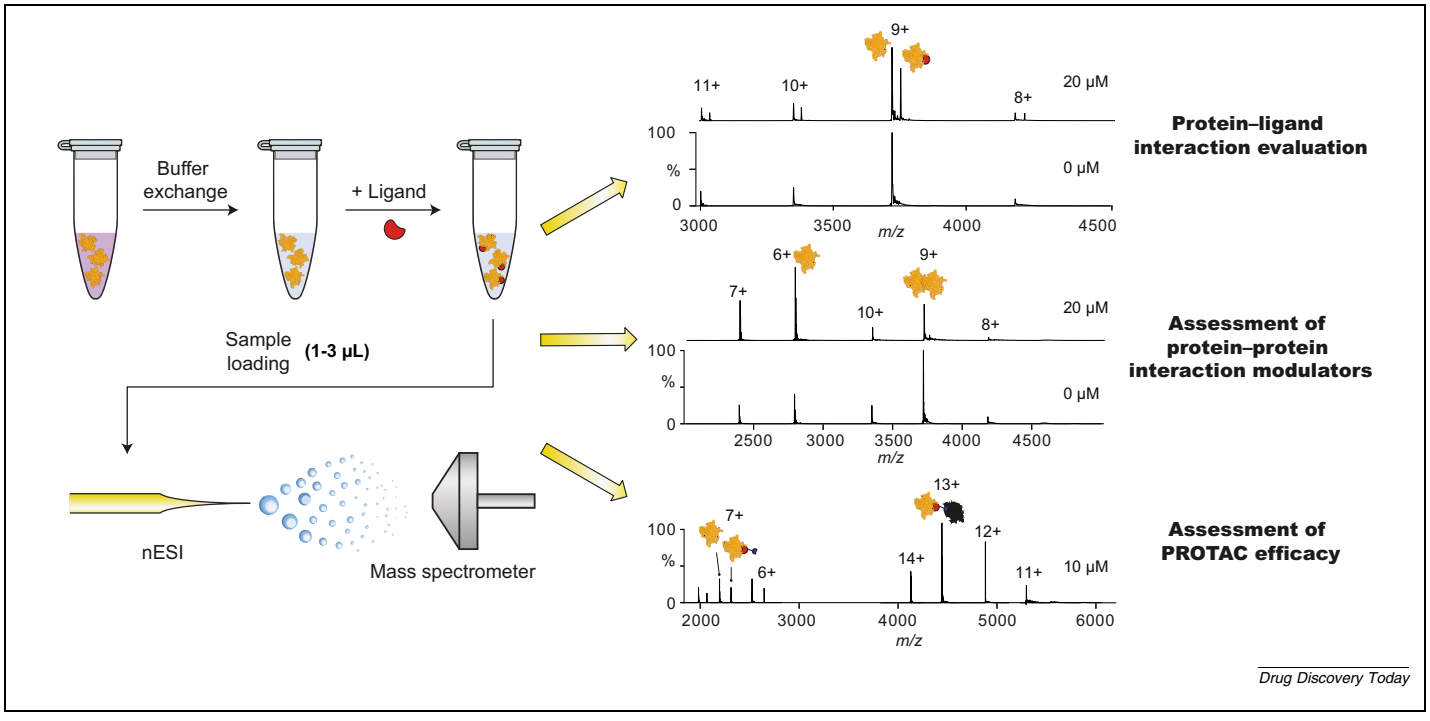

FIGURE 1

Typical workflow for the analysis of ligand binding via native mass spectrometry (nMS). The protein solution is first buffer exchanged into a water solution containing a volatile salt (usually ammonium acetate) using size exclusion chromatography (SEC) or dialysis. This step can be avoided when using nanoscale emitters. The protein is then incubated with increasing concentrations of the ligand of interest, and the mixture is injected into gold-coated emitters for mass spectrometric analysis. The resulting spectra show two peaks, one for the apo protein and one for the ligand-bound complex in the case of protein–ligand binding analysis. In the case of protein–protein interaction (PPI) modulators, the spectra will inform on the influence of the compounds on the assembly of multiprotein complexes. In the case of proteolysis-targeting chimeras (PROTACs), the spectra will show the formation of the protein–PROTAC–E3 ligase ternary complex.

make nESI more amenable for studying protein complexes. In fact, given the smaller orifice, the initial droplet size is at least one order of magnitude smaller, thus reducing the energy and the number of fission events necessary to yield gas-phase ions.[8] Decades of advances in mass analyzers and detectors made it possible to transmit and detect intact proteins. Further developments, including manipulation of pressure gradients within the instruments, enable the preservation of non-covalent interactions in the gas phase within the instrument.[14,15] Moreover, the integration of nMS with multistage tandem MS (MS^n) approaches enables the identification of unknown ligands bound to the target protein. In tandem MS experiments, the precursor ions are mass selected (e.g., in a quadrupole or ion trap) and then subjected to a specific type of activation [e.g., via collision-induced dissociation (CID) or electron-capture dissociation (ECD)]. Following dissociation, the ions are then analyzed according to their m/z. Depending on the used instrument, tandem MS experiments can be performed multiple times, thereby allowing for MS^n experiments, which can then be used to identify ligands dissociated from their protein partners based on their fragmentation pattern. In this regard, ground-breaking work by Klassen *et al.* paved the way for both the evaluation of protein–ligand binding via nMS and the use of MS^n experiments in drug discovery.[16–19]

The main advantages of nMS compared with other biophysical techniques include the absence of any label or protein immobilization, low sample consumption (picomoles of protein are used for each measurement), direct measurement of interactions, and the capacity to distinguish distinct protein species within a heterogeneous population.[9,20] Given these features, nMS is recognized as a highly informative technology for early drug discovery campaigns. In particular, nMS provides assistance for NMR, X-ray crystallography, and cryogenic electronic microscopy (cryo-EM) studies because it allows evaluation of the purity, homogeneity, and integrity of protein samples, as well as the measurement of complicated stoichiometries.[9,21–23]

Similar to other techniques, nMS has not only advantageous properties but also limitations, such as the presence of possible false negatives (gas-phase breakdown of hydrophobic interactions) and false positives (nonspecific binding). These constraints can be solved by optimizing sample preparation or nESI approaches[24–26] and by using appropriate statistical methods to account for nonspecific interactions developing during the nESI process.[16,27]

Overall, nMS complements the existing portfolio of *in vitro* characterization methods and is considered a viable method for identifying, validating, and characterizing hit/lead compounds. This application has been bolstered by advances in instrument technology, which facilitate the examination of bigger, more complicated protein complexes. Indeed, technological advances have resulted in ultra-high mass range spectrometers, which allow for the investigation of complexes formed between small molecules and large proteins, hence expanding the dynamic range of nMS.[28–33] Moreover, the optimization of solubilization methods of membrane proteins is vital for the observation of intact membrane protein complexes in a mass spectrometer,[34–36] and has allowed the analysis of interactions between small molecules and membrane proteins,[29,37–39] including G-protein-coupled receptors (GPCRs).[24,40–42] Finally, nMS coupled with variable temperature nESI enabled the determination of thermodynamic parameters [Gibbs free energy upon binding (ΔG), enthalpy (ΔH), and entropy ($-T\Delta S$)] of protein–ligand interactions and PPIs, which are important parameters to consider during drug development.[43]

In this review, we discuss the most recent applications of nMS for the analysis of protein–ligand interactions, the assessment of PPI modulators, and the evaluation of the so-called 'proteolysis-targeting chimeras' (PROTACs) (Figure 1). We describe the wide applicability of nMS in early drug discovery and highlight the new advancements, future opportunities, as well as challenges of nMS for investigating protein function and modulation (Table 1).

Applications of native MS in drug discovery

Protein–ligand interaction evaluation

nMS coupled to nESI has been widely used to detect and quantify protein–ligand interactions, including small molecules, peptides, and, particularly in the case of membrane proteins, lipids.[22,41,44–48] Nonetheless, care should be taken when analyzing native mass spectra displaying non-covalent protein–ligand interactions and appropriate data analysis and statistical approaches should be used to account for nonspecific interactions arising during the ESI process.[27] For a complete overview of the accurate determina-

TABLE 1

Summary of the advantages and challenges for the different applications of nMS in drug discovery.

Application	Advantages	Challenges
Protein–ligand interaction evaluation	Calculation of K_D values with minimal sample consumption Observation of single binding events and quick identification of allosteric mechanisms Assessment of protein–ligand interactions for multiple compounds in a single experiment	Experiments still relatively low throughput without use of chip-based nESI platforms Possible experimental false negatives (gas-phase breakdown of hydrophobic interactions) or false positives (nonspecific binding)
Assessment of PPI modulators and PROTACs	Observation of protein complex stoichiometry and compound-mediated disruption/stabilization with no need for labeling or immobilization Evaluation of allosteric effects and cooperativity in context of protein oligomerization or multiprotein complex formation Minimal sample consumption	Experiments still relatively low throughput without use of chip-based nESI platforms Multiprotein complexes in equilibrium with their subcomplexes or subunits can yield complex spectra that are difficult to interpret

tion of protein–ligand interactions using nMS, we refer the reader to recent reviews by Bennett and colleagues[49] and Gavriilidou *et al.*, with the latter focusing primarily on high-throughput nMS for drug screening.[50]

nMS can successfully evaluate protein–ligand interactions in a reasonably medium-throughput way (~100 ligands per hour) using a procedure known as bioaffinity MS. This approach involves the incubation of a ligand or combination of ligands with a protein of interest, with the resultant solution being examined directly by nMS. The identification of bound small molecules may be determined easily by measuring the difference in the mass-to-charge ratio (m/z) between the ligand-bound and apo protein peaks (Figure 1). The use of nMS for compound library screening is gaining increasing interest, as exemplified by the studies by Vu *et al.*[51] and Nguyen *et al.*,[52] which we discuss below. Hence, chip-based automated nESI platforms, such as the NanoMate,[53] are being increasingly used because they provide constant nESI conditions and greater reproducibility, along with augmented throughput. An example of this approach was provided by Vu *et al.*, who applied nMS to screen a library of natural product fragments against 62 *Plasmodium falciparum* proteins selected as potential malaria drug targets. Each protein was incubated with fragments at ligand:protein molar ratios varying from 5:1 to 20:1. This approach enabled the identification of 96 potential binders, which formed complexes with 32 proteins. The 96 natural product fragments had different chemotypes and were different from the known antimalarial aminoquinolines, quinolones, or diamidines. Interestingly, the technique managed to distinguish between promiscuous and nonpromiscuous pan-assay interference compounds (PAINS), such as polyphenols, epoxides, Michael acceptors, and β-lactams, thereby confirming the ability of nMS to capture specific interactions.[51]

More recently, Nguyen and coworkers integrated nMS and untargeted metabolomics to develop a method to identify natural products that interact with potential drug targets.[52] Specifically, they incubated crude natural product extracts containing thousands of small molecules with the target proteins and applied a quick, low-volume gel filtration step using 0.5-ml desalting columns to remove unbound ligands. This was followed by nMS analysis to capture and quantify protein–ligand interactions (Figure 2a) and by the identification of the bound hits through metabolomics. To do so, they used nanoscale nESI emitters (internal diameter of ~250 nm), which, differently from the widely used microscale emitters, are tolerant of the presence of salt and enable the analysis of complex mixtures, such as those containing thousands of natural products.[25] Through this approach, the authors identified novel and known binders of human carbonic anhydrases (hCA), a family of metalloenzymes that catalyze CO_2 hydration,[54] which is attracting attention because it is implicated in the initiation and progression of several pathologies, including cancer.[55] To determine the identity of the bound ligands, they performed MS^n analysis with a linear ion trap (Figure 2a). This approach, already exploited for the identification of ligands bound to either soluble or membrane proteins,[28,56] involved the isolation of the ligand-bound protein followed by dissociation and fragmentation of the ligand to gain a fragmentation spectrum (Figure 2a). This led to identification of 1,2,3,4,6-penta-*O*-galloyl-β-D-glucose (Figure 2b) as a new ligand of hCAI and the binding was later confirmed in nMS-based titration experiments, yielding a K_D value of 27 μM.[25]

Agasid *et al.* also used nanoscale nESI emitters (internal diameter of ~100 nm) for the analysis of GPCRs in buffers containing high concentrations of sodium ions.[24] This allowed for the detection of adenosine 2A receptor (A2AR) in lauryl maltose neopentyl glycol (LMNG) detergent micelles bound to up to seven sodium ions, as well as investigation of the effects of A2AR agonists (NECA and CGS21680) and antagonists (XAC and ZM241385) on sodium binding. Indeed, whereas both agonists abolished protein–sodium ion interaction, this was instead retained in the presence of both antagonists, in line with solution-based studies in which only inactive conformations maintain sodium ions in the allosteric binding pockets.[57] The glucagon receptor was successfully observed in mixed micelles containing the recently developed first-generation, dendritic oligoglycerol detergent (G1)[35,42] and cholesteryl hemisuccinate. The authors captured glucagon binding, whereas no sodium adducts were observed this time. They also observed the binding of the negative allosteric modulator NNC0666, which had been added during purification to stabilize the protein and the identity of which was confirmed via MS^n on a Orbitrap-Ion Trap mass spectrometer.

Another interesting method used for the quantification of protein–ligand affinities was described by Ren and coworkers, who developed an online SEC-nMS platform (Figure 2c). Through this procedure, they calculated the K_D values for the interaction of small-molecule inhibitors with the catabolic enzyme indoleamine 2,3-dioxygenase 1 (IDO1)[58] and these values were in line with chip-based[53] nESI-nMS measurements. To do so, they incubated IDO1 with increasing concentrations (0.5–100 μM) of different ligands, followed by a 3-min SEC run coupled to a nESI-nMS system (Figure 2d, upper-left panel). Furthermore, one-shot competition experiments by mixing IDO1 with an equimolar mixture of two potential binders (called compounds **1** and **2** in the paper) indicated a higher abundance of IDO1-**1** adducts (Figure 2d, upper-right panel), in line with K_D calculations. In addition, the authors analyzed protein–ligand interactions in the gas phase by performing in-source CID experiments. These are executed by increasing the collision voltage until full complex dissociation, allowing calculation of the VC_{50} parameter (i.e., the collision voltage required to dissociate the protein–ligand complex by 50%), which was found to be independent from the protein:ligand ratio. Moreover, a higher VC_{50} value was obtained for the more tightly bound ligand (compound **1**), thus being in line with the measured K_D values (Figure 2d, lower panels). Overall, this method enabled accurate measurements in this system, with the main advantages relying on the automation and rapidity of the analysis and the minimization of the residence time in ammonium acetate. By contrast, assessment of weak interactions might be hindered in cases in which the dissociation rate is fast enough to occur during the chromatographic separation.

nMS has also been applied in conjunction with fluorescence thermal shift assays for the identification of new ligands of the serine/threonine kinase c-Jun *N*-terminal kinase 3 (JNK3).[59] Following identification of seven potential hits through fluorescence thermal shift (FTS) assays, nMS was used to calculate the

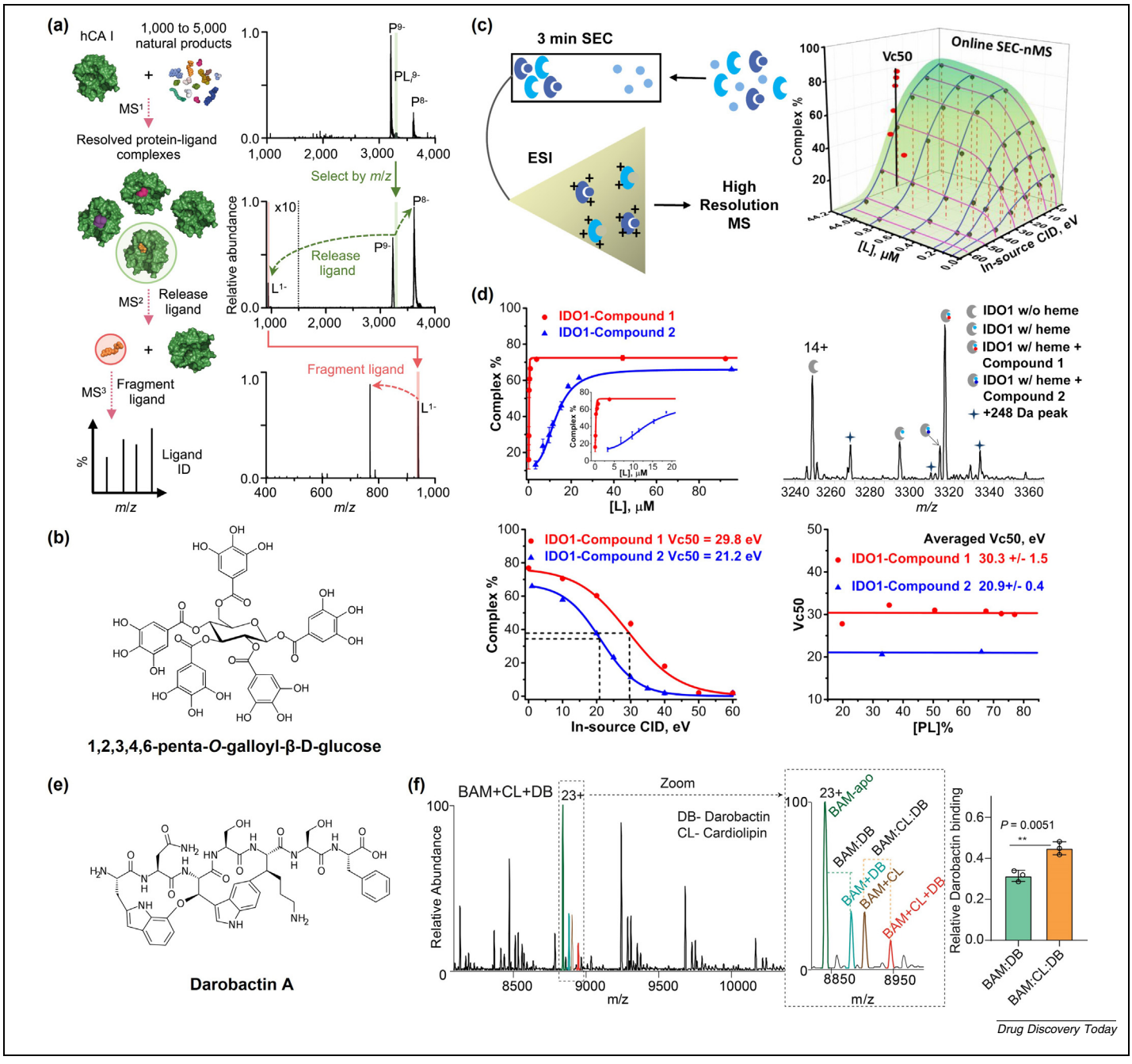

FIGURE 2

Evaluation of protein-ligand interactions. **(a)** Schematic indicating the key steps necessary for the identification of small molecules bound to the target protein via native mass spectrometry (nMS) following incubation with extracts containing thousands of natural products. **(b)** Structure of **1,2,3,4,6-penta-*O*-galloyl-β-D-glucose**. **(c)** Schematic of workflow used for size exclusion chromatography (SEC)-nMS. **(d)** Evaluation of the binding affinity between IDO1 and two small molecules via SEC-nMS (upper panels) along with measurement of the VC_{50} constant and demonstration that the VC_{50} value is independent from the protein:ligand ratio (lower panels). **(e)** Structure of **darobactin A**. **(f)** Mass spectra of the β-barrel assembly machinery (BAM) complexes in the presence of both cardiolipin (CL) and darobactin (DB) (left panel). Central panel: expansion of the 23+ charge state to focus on CL, darobactin, and CL + darobactin binding to BAM. Right panel: quantification of the darobactin-bound peak intensities relative to the corresponding darobactin-free species. Adapted, with permission, from [52] (a), [58] (d), and [66] (f).

binding affinities of these compounds, which have a diverse subset of scaffolds, including *N*-(1H-pyrazol-4-yl)thieno[2,3-d]pyrimidin-4-amine (four compounds), 5-(phenylamino)-1*H*-1,2,3-triazole-4-carboxamide (one compound), triazolmethypiperidine (one compound), and piperidinecarboxamide (one compound). nMS successfully captured protein–ligand interactions for four of these compounds, with **5**, bearing a 5-(phenylamino)-1*H*-1,2,3-triazole-4-carboxamide core, being the most tightly bound ligand, with a K_D value of 21 μM.

Recently, D'Amico *et al.* described an ion mobility-nMS (IM-MS) method coupled to droplet microfluidics for analyzing protein–ligand interactions by assessing the influence of ligand

binding on protein stability in the gas phase.[60] Before mass spectrometric analysis, IM enables the separation of protein ions based on their size and shape within a drift tube filled with neutral gas under the influence of a weak electric field. The time that it takes for an ion to travel through the drift tube is proportional to its collision cross-section (CCS), which refers to the rotationally averaged projection area of the ion.[61] Following optimization of the microfluidics system for sample introduction in the mass spectrometer, the authors performed collision-induced unfolding (CIU) assays on the protein lysine deacylase SIRT5, a promising target for the development of modulators that could serve as potential drugs in many pathologies.[62–64] CIU experiments, comprising analysis of the change in drift time in the IM cell as a function of collision voltage, enable the detection of subtle changes in protein structure and stability.[65] In the case of SIRT5, CIU fingerprints indicated the presence of three different states and two transition regions, corresponding to a compact native-like structure and two unfolded states accessed during the CIU experiment. Hence, CIU experiments were used to screen a small library of 96 small molecules against SIRT5. These assays are based on the notion that compound binding to the target protein increases its stability and, thus, higher voltages would be necessary to unfold the protein. This screen identified 24 compounds capable of increasing the median collision voltage necessary to reach both CIU transitions (CIU_{50}s), indicating that these molecules exert a stabilizing effect on SIRT5. Five of these molecules were also tested for their inhibitory potency, with the compounds exhibiting the greatest SIRT5 inhibitory activity also causing the largest shifts in CIU_{50} for the first transition, whereas the opposite trend was observed for the second transition. Based on the assumption that these compounds are SIRT5-competitive inhibitors (although no data were reported in the paper), the authors suggested that the first transition represents the unfolding of the substrate binding domain, while the second transition may represent the unfolding of SIRT5 Zn^{2+}-binding domain. However, further research will be required to corroborate these claims. Although this technology decreases data acquisition time and sample consumption, a significant decrease in sensitivity was found owing to the increased flow rates and emitter sizes necessary for interfacing with the microfluidic platform. Overall, these authors presented a novel method for screening small molecules against protein targets, and it would be interesting to extend its application to other protein systems.

An intriguing example of the application of nMS to membrane protein–ligand binding as provided by Kaur *et al.*, who captured the interaction between the β-barrel assembly machinery (BAM) complex and the recently discovered peptide-based antibiotic darobactin A (Figure 2e).[66] The BAM complex, which comprises five subunits, including the outer membrane (OM) protein BamA and the lipoproteins BamB–E, promotes the folding and insertion of OM proteins in the OM of Gram-negative bacteria. nMS experiments indicated that the BAM complex preferentially interacts with negatively charged lipids, such as phosphatidylglycerol (PG) and cardiolipin (CL). Interestingly, CL binding to the BAM complex was shown to enhance its affinity for darobactin A, as demonstrated by the spectra indicating that darobactin preferentially binds to Bam-CL compared with the apo BAM complex (Figure 2f).

Finally, nMS has also been applied for the analysis of protein–ligand interactions directly from cell lysates and enabled evaluation of overexpressed proteins directly from crude samples without purification.[67] Rogawski and colleagues applied this approach to the kinase domain of Bruton's tyrosine kinase (BTK_KD) overexpressed in HEK293T cells. They first incubated BTK_KD-overexpressing cells with either the covalent drug ibrutinib or its non-covalent counterpart, ibrutinib-NH_2, then resuspended the cell pellets in 150–300 mM ammonium acetate and lysed the resulting suspension, which was centrifuged and further diluted before nMS analysis. Through this method, the authors captured the interaction between BTK_KD and both ibrutinib and ibrutinib-NH_2. The same approach was then translated to other BTK ligands (pluripotin, LY2409881, vemurafenib, and PP-121) and enabled the authors to rank their binding affinities, with pluripotin being the tightest binder. Overall, this method has the potential to be used to validate hit/lead compound cellular target engagement, although it still requires protein overexpression, which could alter the physiological state of the studied cellular system and impair off-target binding identification. Nonetheless, it is a promising orthogonal approach to conventional assays, such as in-cell NMR and cellular thermal shift assays (CETSA), because, unlike these assays, it allows for direct observation of protein–ligand binding and could be used to evaluate drug combinations. Along the same line, Olinares *et al.*[68] previously described a workflow that enables the analysis of protein assemblies directly from cell lysates, without the requirement for overexpression, by combining affinity isolation with antibody-conjugated beads and nMS. Therefore, it would be intriguing to combine the methods described by Rogawski *et al.* and by Olinares *et al.* to explore the influence of small molecules on protein complexes.

Assessment of protein–protein interaction modulators

nMS has also been extensively used for evaluation of both disruptors and stabilizers of PPIs. To this end, the Robinson group applied nMS to both soluble and membrane proteins to clarify the mode of action of known drugs and to support the development of novel potential PPI disruptors.[69–71] For instance, this approach was applied by Fiorentino and coworkers to the *Pseudomonas aeruginosa* lipopolysaccharide (LPS) transport (Lpt) protein LptH to gain insights into its monomer/dimer equilibrium and PPI disruption via small molecules.[69] The Lpt system is a multiprotein complex formed by seven different proteins responsible for LPS transport from the inner membrane to the OM.[72] Among them, the periplasmic protein LptA forms an oligomeric bridge connecting the two membranes and is pivotal for the translocation pathway. In the multidrug-resistant opportunistic pathogen *P. aeruginosa*, the ortholog of LptA, LptH, forms dimers in solution.[73] Using nMS, the authors quantified the monomer–dimer equilibrium of LptH and assessed the potency and efficacy of the antimicrobial peptide thanatin and small-molecule disruptors, obtaining information on their structure–activity relationships (SARs). Specifically, nMS experiments indicated that LptH exists mainly as a dimer, which is disrupted by thanatin as well as the known LPS transport inhibitor IMB-881.[69] Based on its structure, the authors evaluated a library of 5-carboxy-8-hydroxyquinoline derivatives bearing a small acyl side chain.

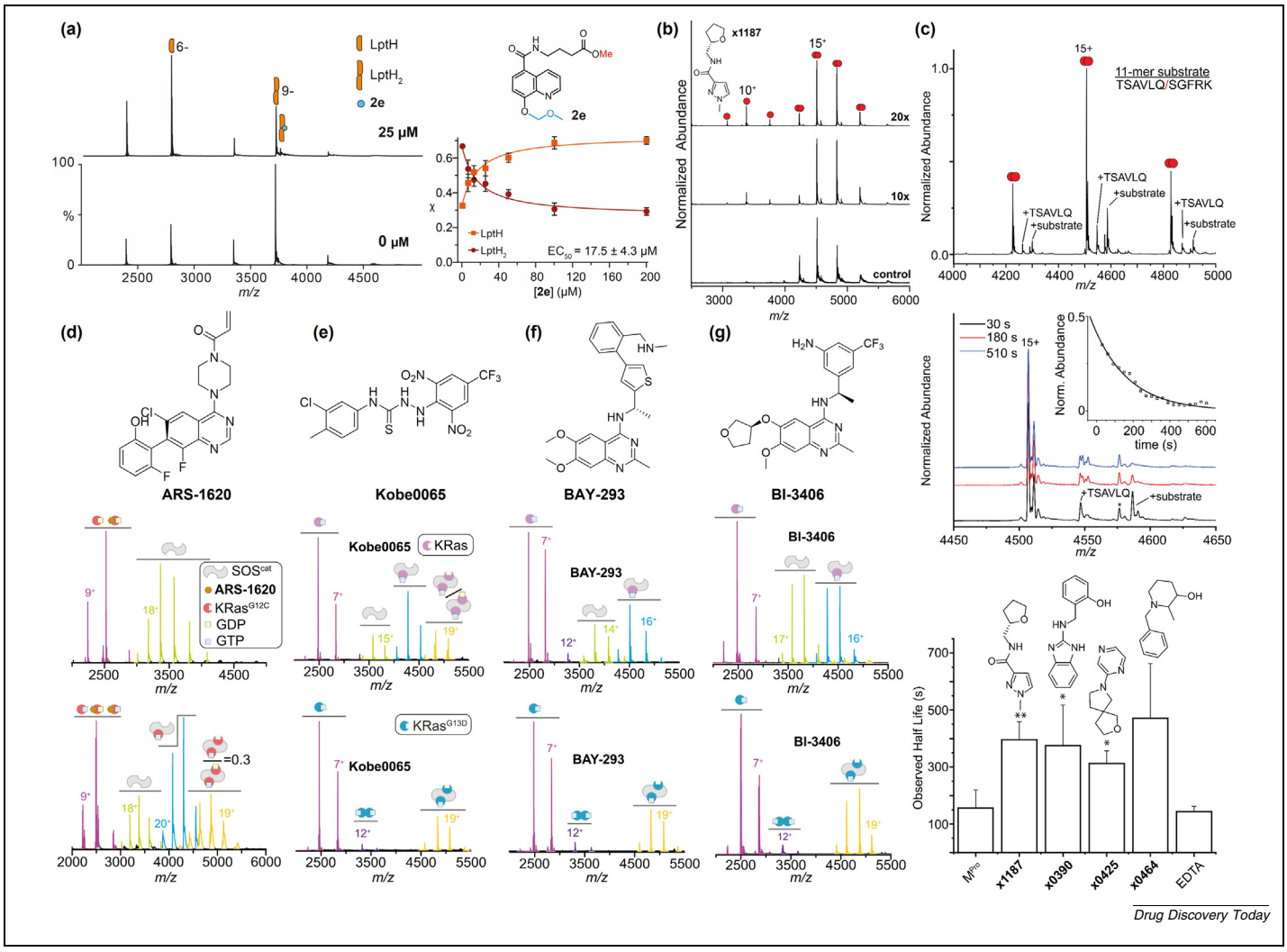

FIGURE 3

Assessment of protein-protein interaction (PPI) disruptors. **(a)** Mass spectra showing the effect of the quinoline derivative **2e** on LptH monomer/dimer equilibrium and relative quantification (right panel). **(b)** Native mass spectra of M^{pro} (5 μM) in the presence of increasing equivalents of **x1187**. **(c)** Upper panel: native mass spectrum of M^{pro} (5 μM) in the presence of the 11-mer substrate (50 μM) at t = 30 s. Peaks labeled 'TSAVLQ' and '+substrate' indicate acyl–enzyme complex and the non-covalent enzyme–substrate complex, respectively. Central panel: mass spectra of the 15+ charge state at three representative times showing the substrate cleavage reaction. Inset: plot of the relative abundance of the enzyme-substrate complex as a function of time. Lower panel: bar chart indicating the half-lives of the enzyme-substrate complex in the presence of the tested small molecules. **(d)** Structure of **ARS-1620** (upper panel). Mass spectra recorded following addition of **ARS-1620** (10 μM) to preincubated mixtures of 1 μM SOS^{cat} with 3 μM of $KRas^{G12C}$–GDP (central panel) or $KRas^{G12C}$–GTP (lower panel). **(e)** Structure of **Kobe0065** (upper panel). Mass spectra recorded following addition of **Kobe0065** (2.5 μM) to preincubated mixtures of 1 μM SOS^{cat} with 3 μM KRas–GTP (central panel) or $KRas^{G13D}$–GTP (lower panel). **(f)** Structure of **BAY-293** (upper panel). Mass spectra recorded following addition of **BAY-293** (2.5 μM) to preincubated mixtures of 1 μM SOS^{cat} with 3 μM KRas–GTP (central panel) or $KRas^{G13D}$–GTP (lower panel). **(g)** Structure of **BI-3406** (upper panel). Mass spectra recorded following addition of **BI-3406** (2.5 μM) to preincubated mixtures of 1 μM SOS^{cat} with 3 μM KRas–GTP (central panel) or $KRas^{G13D}$–GTP (lower panel). Peaks corresponding to KRas, SOS^{cat}, binary, and ternary complexes are colored in purple, chartreuse, cyan, and orange, respectively. Adapted, with permission, from [70] (c) and [76] (f).

nMS experiments revealed that short (up to five carbons) acyl chains had higher disruption activity, and that protecting carboxyl and hydroxyl groups via methylation and methoxymethylation, respectively, increased compound activity (Figure 3a).[69] This study presented a new method for evaluating LptA/H PPI disruptors and led to the identification of new quinoline-based hit compounds, which represent the basis for the development of novel LPS transport inhibitors.

A similar approach was used to evaluate the effects of allosteric inhibitors on the dimerization of the severe acute respiratory syndrome-coronavirus 2 (SARS-CoV-2) main protease (M^{pro}). M^{pro} is the enzyme responsible for cleaving along the two viral polypeptides to release the nonstructural proteins necessary for replication. Through nMS, El-Baba *et al.* showed that M^{pro} is preferentially a dimer in solution and then analyzed the effect of four fragments[74] on the monomer–dimer equilibrium.[70] Notably, one compound (x1187), which had been indicated to bind to the dimer interface,[74] was shown to disrupt the dimeric assembly (Figure 3b). Conversely, the three remaining compounds, which had previously been shown to interact with a solvent-exposed surface,[74] had no effect on M^{pro} dimerization. Further nMS-based kinetic experiments indicated that the frag-

ments could increase the lifetime of the enzyme–substrate complex, thereby slowing the rate of substrate processing by up to 40% (Figure 3c).[70] This work highlights the versatility of nMS, which was used to acquire thermodynamic and kinetic information on the effects of small molecules on the monomer–dimer equilibrium and enzymatic processing. More recently, Zhu *et al.* used a nMS-based bioaffinity selection method to screen for small molecules obtained from crude herbal extracts against M^{pro}.[75] They identified the three flavonoids (baicalein, scutellarein, and ganhuangenin) as M^{pro} ligands with K_D values in the low micromolar range. These compounds did not alter the dimeric assembly of M^{pro}, but could still inhibit its enzymatic activity, with IC_{50} values in line with the measured K_Ds.

Moghadamchargari and coworkers recently used nMS to investigate interactions between the oncoprotein KRas and the catalytic domain of the guanine nucleotide exchange factor Son of Sevenless (SOS^{cat}), which is responsible for reloading KRas with GTP.[76] The KRas isoform investigated was human KRas4B (residues 1–169), referred to as KRas for the sake of simplicity. The authors investigated the binding of SOS^{cat} to wild-type KRas, as well as three oncogenic mutants (G12C, G13D, and Q61H). In this context, they examined the effect of the covalent $KRas^{G12C}$ inhibitor ARS-1620[77] and three known small-molecule KRas–SOS disruptors (Kobe0065,[78] BAY-293,[79] and BI-3406[80]) on the interaction between SOS^{cat} and different KRas variants (Figure 3d–g). The authors demonstrated that ARS-1620 could react with GDP-loaded $KRas^{G12C}$, but showed limited reactivity in the presence of GTP (Figure 3d). In line with this, ARS-1620 could disrupt the $KRas^{G12C}$–GDP/SOS^{cat} complex, but was ineffective against the $KRas^{G12C}$–GTP/SOS^{cat} association (Figure 3d). Kobe0065 (IC_{50} = 20-μM), reported as a KRas-GTP ligand,[78] was unable to disrupt the KRas–GTP or $KRas^{G12D}$–GTP interactions with SOS^{cat} (Figure 3e) and could not abolish SOS^{cat} binding to $KRas^{G12C}$. Different from Kobe0065, BAY-293 (IC_{50} = 21 nM) and BI-3406 (IC_{50} = 5 nM) have been reported to bind directly to SOS^{cat}.[79,80] BAY-293 could not disrupt the SOS^{cat} interaction with either KRas–GTP (Figure 3f, middle panel), $KRas^{G12C}$–GTP, or $KRas^{G12D}$–GTP (Figure 3f, lower panel), whereas it was effective for unloaded KRas and $KRas^{G12C}$. Similarly, BI-3406 (tested at 2.5 μM) acted as a KRas/SOS^{cat} disruptor (Figure 3g, middle panel) but could not disrupt the $KRas^{G12D}$/SOS^{cat} interaction (Figure 3g, lower panel) and was effective only at 20 μM, 4000× its reported IC_{50}. This study not only advanced our understanding of KRas/SOS interactions, but also provided key insights into the modes of action of known KRas/SOS disruptors, none of which were effective in the presence of GTP-loaded KRas. Overall, this report exemplifies the power of nMS in clarifying drug modes of action, thereby providing a foundation for the development of optimized modulators.

Bolla *et al.* elucidated the influence of chlorhexidine, a common antiseptic, on the oligomerization of the chlorhexidine efflux pump AceI from *Acinetobacter baumannii* and on its transcriptional regulator AceR.[71] nMS experiments demonstrated that AceI exists in a pH-dependent monomer–dimer equilibrium, with the functional form being the dimeric AceI. Interestingly, this equilibrium is altered by chlorhexidine, which increases AceI dimer formation, thereby facilitating the functional form of the efflux pump. Further nMS experiments revealed that the transcriptional regulator AceR exists mostly as a dimer, although a small fraction of tetramers is also present in solution. nMS data also showed that *A. baumannii* RNA polymerase constitutively binds the promoter region upstream of *AceI*. When AceR was introduced into the system, its dimeric form competitively interacted with the DNA fragment, inhibiting the RNA polymerase promoter binding, thus impairing AceI transcription. Interestingly, chlorhexidine addition increased the amount of tetrameric AceR, which is unable to interact with DNA, thereby allowing RNA polymerase to bind the promoter and start transcription.[71] Overall, by assessing the influence of small molecules on protein–protein and protein–nucleic acid interactions, nMS revealed crucial insights into the mechanism of antibiotic drug resistance. This approach could be expanded to the identification of small molecules acting either as AceI dimerization disruptors or as antagonists of the AceR–chlorhexidine interaction, therefore contributing to the discovery of novel antibacterial agents for the treatment of chlorhexidine-resistant bacteria infections.

Bellamy-Carter and coworkers recently used nMS to investigate the influence of different small molecules acting as stabilizers of the interactions between the eukaryotic regulatory protein 14-3-3σ and three of its binding partners: the tumor suppressor p53, the leucine-rich repeat kinase 2 (LRRK2), and the estrogen receptor α (ERα).[81] nMS experiments demonstrated that 14-3-3σ is a dimer with the highest affinity for ERα followed by LRRK2 and p53 (Figure 4a–c, upper panels). The fungal diterpenoid glycoside fusicoccin A (Figure 4d), known to stabilize the interactions between 14-3-3σ and its partners to a different extent,[82–84] was shown to further increase the abundance of the 14-3-3σ/ERα complex. while having little or no effect in the case of p53 and LRRK2, respectively (Figure 4a–c). Interestingly, the nMS spectra revealed that the fusicoccin A effect increased in the presence of a higher ERα concentration, thereby suggesting a cooperative binding mode, whereby fusicoccin A preferentially interacts with the 14-3-3σ/ERα complex rather than with the single subunits. Finally, the authors screened a drug cocktail of potential 14-3-3σ PPI stabilizers. Incubation of 14-3-3σ/ERα with a cocktail of seven different molecules indicated that the only compound able to stabilize the interaction is fusicoccin A and, to a lesser extent, its biosynthetic deacetoxy precursor fusicoccin J. This work highlights the utility of nMS as a screening approach for PPI stabilizers because it can not only provide a measurement of their potency, but also enable elucidation of subtle aspects, such as cooperative binding.

Recent work by Yen *et al.*, resulting from a collaboration between Oxford University and OMass Therapeutics scientists, exemplified the ability of nMS to capture the effects of ligand binding to the turkey β_1-adrenergic receptor ($t\beta_1AR$), which influence its coupling to different G proteins.[85] Initial measurements performed at a ligand:$t\beta_1AR$ 50:1 molar ratio enabled the derivation of significant SARs by demonstrating that isoprenaline could induce 100% complex formation between $t\beta_1AR$ and an engineered mini-G stimulatory (mini-G_s) protein, whereas compounds lacking the essential moieties for receptor binding were less effective (Figure 4e, upper panel). Among these derivatives, orciprenaline, in which the *para*-hydroxy group of isoprenaline is moved to the *meta* position, displayed a 60% reduction in mini-G_s coupling. Similarly, 1-phenyl-2-(2-propylamino)ethan-1-ol, lacking both the catechol hydroxy groups, abolished 90%

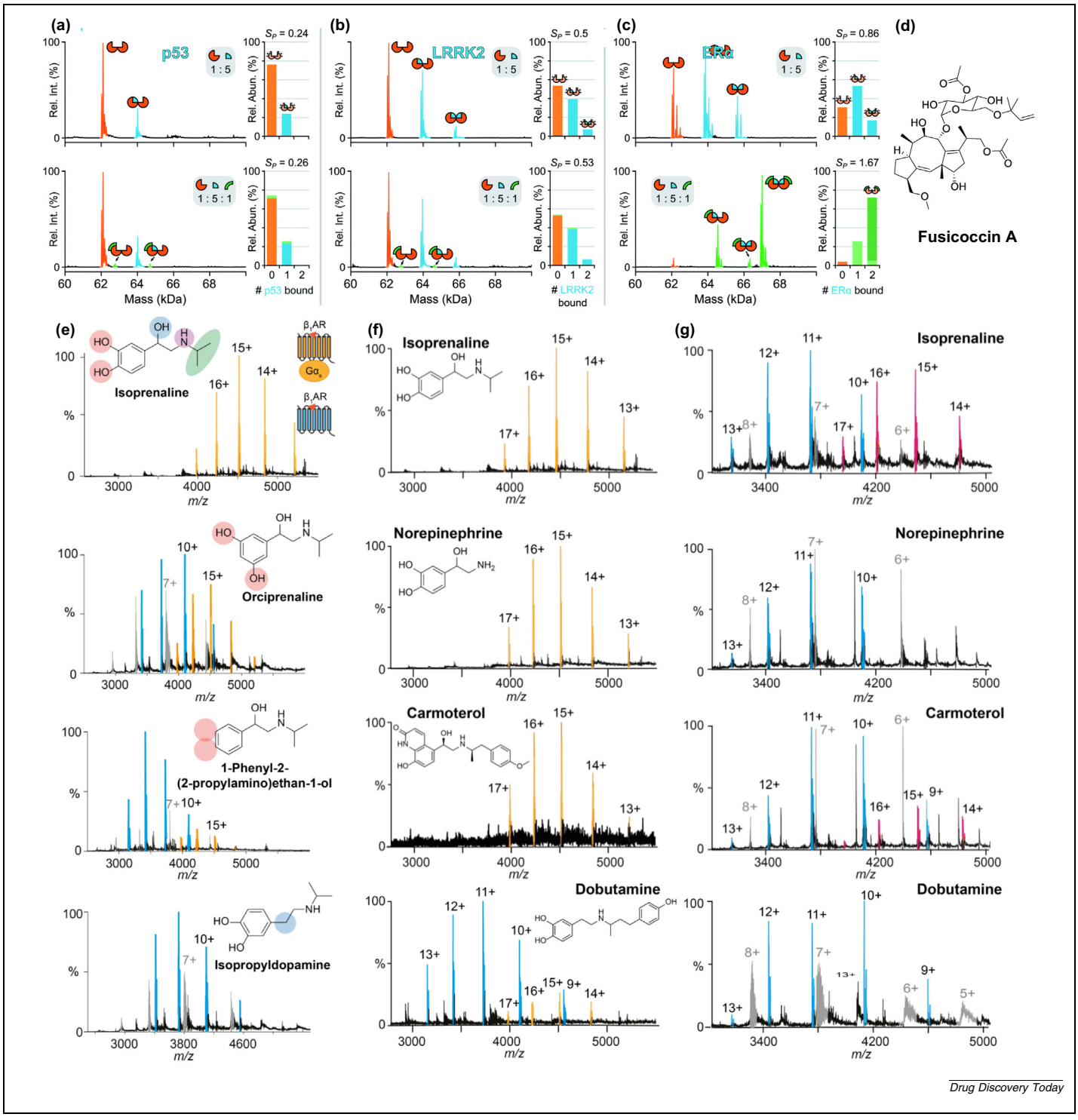

FIGURE 4

Assessment of protein-protein interaction (PPI) stabilizers. **(a)** Structure of **fusicoccin A**. **(b–d)** Deconvoluted mass spectra showing the interaction between 14-3-3σ (monomer concentration 5 μM) and each interacting partner [p53 (b), leucine-rich repeat kinase 2 (LRRK2) (c), and estrogen receptor alpha (Erα) (d), 25 μM] in the absence or in the presence of 5 μM **fusicoccin A**. Bar charts show the stoichiometry of the PPIs detected by native mass spectrometry (nMS). **(e)** Mass spectra showing the interaction between tβ_1AR (5 μM) and mini-G_s (6 μM) in the presence of **isoprenaline**, **orciprenaline**, **1-phenyl-2-(2-propylamino)ethan-1-ol**, and **isopropyldopamine** (250 μM). **(f–g)** Mass spectra showing the interaction between tβ_1AR (5 μM) and mini-G_s (f) or mini-$G_{i/s}$ (g) (6 μM) in the presence of the full agonists **isoprenaline**, **norepinephrine**, **carmoterol**, and the partial agonist **dobutamine** (25 μM). The peaks assigned to tβ_1AR-mini-G_s complex, tβ_1AR, mini-G_s, and tβ_1AR-mini-$G_{i/s}$ complex are depicted in orange, blue, gray, and magenta respectively. The structures of each compound are indicated alongside each spectrum. Adapted, with permission, from [81] (b–d) and [85] (e–g).

mini-G_s coupling (Figure 4e, central panels). Moreover, isopropylldopamine, lacking the β-hydroxy group, completely abolished mini-G_s coupling (Figure 4e, lower panel). Further nMS experiments performed at a ligand:tβ_1AR 5:1 molar ratio recapitulated the effects of full agonists (isoprenaline, norepinephrine, and carmoterol), partial agonists (dobutamine and salbutamol), and antagonists (cyanopindolol, carazolol, and carvedilol) by showing that full agonists are capable of inducing 100% tβ_1AR-mini-G_s complex formation, whereas partial agonists were less effective, and antagonists could not enable mini-G_s coupling (Figure 4f). In addition, experiments in the presence of mini-$G_{i/s}$ protein [in which the helix 5 motif of mini-G_s was replaced with the sequence of the G inhibitory (G_i) protein] enabled the assessment of agonist-biased signaling. nMS data showed that isoprenaline could induce mini-$G_{i/s}$ coupling, whereas carmoterol was less effective and norepinephrine could not stimulate mini-$G_{i/s}$ coupling at all (Figure 4g). Competition experiments in the presence of both mini-G_s and mini-$G_{i/s}$ further demonstrated that isoprenaline preferentially induces mini-G_s coupling. Interestingly, the authors also showed that Zn^{2+} has a key role in stabilizing the tβ_1AR-mini-G_s complex formation. In line with this, treatment with the divalent cation chelator ethylenediaminetetraacetic acid (EDTA) abolished tβ_1AR–mini-G_s interactions, which were reinstated by treatment with $ZnCl_2$.

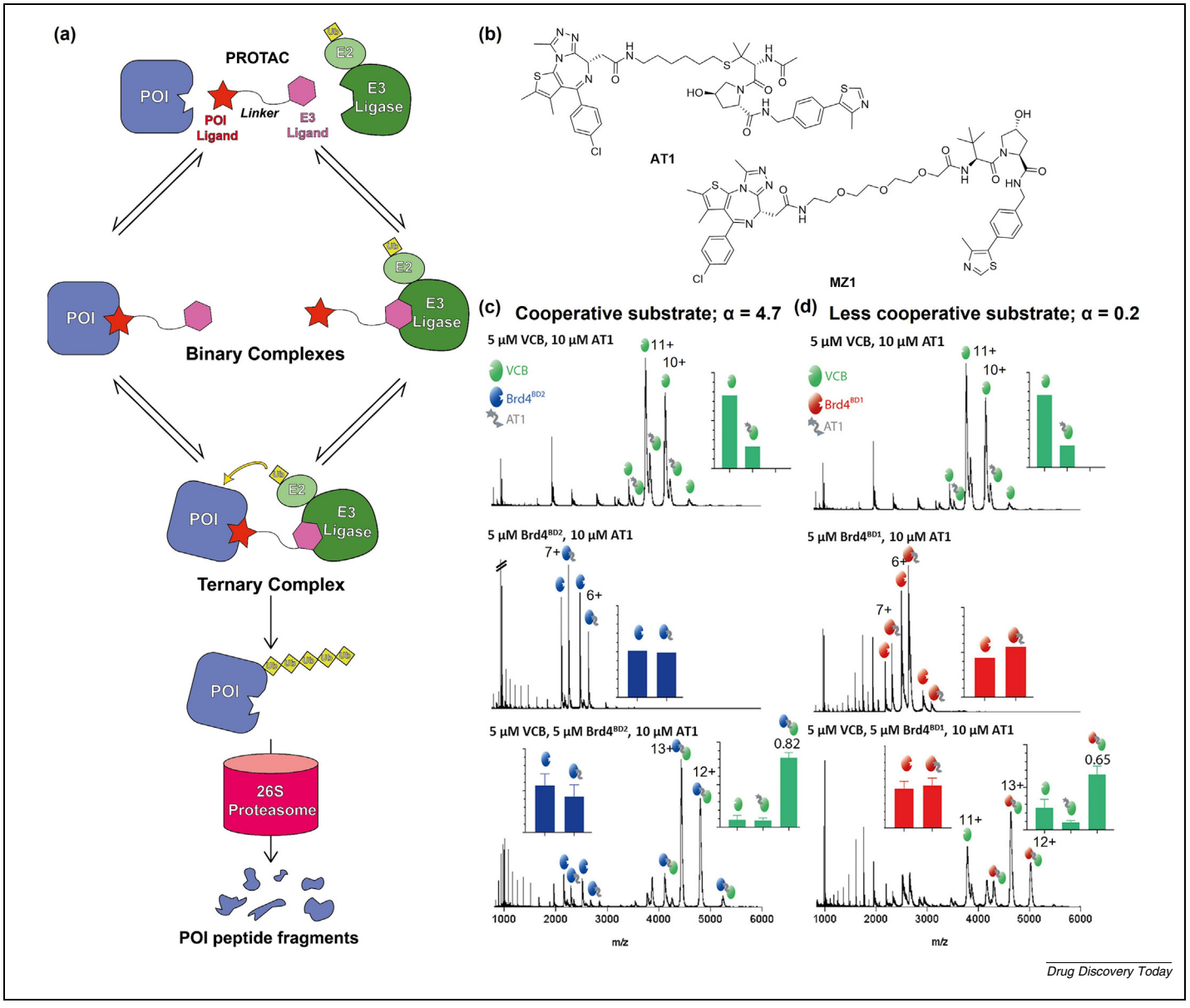

FIGURE 5

Evaluation of proteolysis-targeting chimeras (PROTACs). **(a)** Schematic of the protein degradation mechanism promoted by PROTACs. By interacting with an E3 ligase and the protein of interest (POI), PROTACs physically bring the two proteins into proximity, thereby promoting POI ubiquitination and consequent proteasomal degradation. **(b)** Structures of the VHL-recruiting PROTACs **AT1** and **MZ1**. (c) Mass spectra showing the interaction between the VCB complex (5 μM) and **AT1** (10 μM) (upper panel); $Brd4^{BD2}$ (5 μM) and **AT1** (10 μM) (central panel); and VHL/elongin-B/elongin-C (VCB) (5 μM), **AT1** (10 μM), and $Brd4^{BD2}$ (5 μM) (lower panel). Bar charts provide the quantification of the relative abundance of each species. **(d)** Mass spectra showing the interaction between VCB (5 μM) and **AT1** (10 μM) (upper panel); $Brd4^{BD1}$ (5 μM) and **AT1** (10 μM) (central panel); and VCB (5 μM), **AT1** (10 μM), and $Brd4^{BD1}$ (5 μM) (lower panel). Bar charts provide the quantification of the relative abundance of each species. Adapted from [87] (c,d).

Molecular dynamics (MD) suggested that Zn^{2+} ions promote the structural transition during the formation of complexes between G-proteins and receptors, and subsequent site-directed mutagenesis studies showed that $t\beta_1AR$ mutants with decreased Zn^{2+} binding were also characterized by reduced mini-G_s coupling. In this study, no protein–drug interactions were detected because the voltages used to enable the liberation of $t\beta_1AR$ from detergent micelles led to dissociation of the small molecules. Nonetheless, this study demonstrates the ability of nMS to guide drug design by monitoring the effect of potential drugs on specific pharmacological pathways (e.g., GPCR–G-protein coupling) rather than directly detecting protein–ligand interactions.

Assessment of PROTAC efficacy

PROTACs are heterobifunctional molecules constituted by an E3 ligase-recruiting moiety connected via a linker to a warhead that binds the protein of interest (POI). PROTACs bring an E3 ligase and a POI into proximity, thus promoting POI polyubiquitination and proteasomal-mediated degradation, and are then released and recycled to induce the degradation of a new POI (Figure 5a), displaying a catalytic mode of action.[86] Compared with classical inhibitors, they usually show higher potency and selectivity, prolonged pharmacodynamic effects, and the ability to evade most resistance mechanisms based on target mutations. The most targeted E3 ligases are Cereblon, usually targeted by thalidomide and derivatives, and the Von Hippel–Lindau protein (VHL), usually targeted by the small-molecule VH032 and related compounds.[86]

Over the years, specialized protocols in biochemical and biophysical methods have been devised to characterize the formation of the POI–PROTAC–E3 ligase ternary complex to assess *in vitro* the potential of PROTACs. These include ITC and SPR, which provide key information on the thermodynamics and kinetics of PROTAC binding. More recently, nMS has been indicated as a powerful tool to capture POI–PROTAC–E3 ligase ternary complex formation. Through nMS, Beveridge *et al.* captured the interaction between the E3 ligase complex VHL/elongin-B/elongin-C (VCB), a bromodomain and extra-terminal domain (BET) protein ($Brd3^{BD2}$, $Brd4^{BD1}$, or $Brd4^{BD2}$) and the PROTACs AT1 and MZ1 [the POI ligand of which is the pan-BET inhibitor (+)-JQ1] (Figure 5b).[87] Native mass spectra indicated that both AT1 and MZ1 preferentially form a ternary complex with $Brd4^{BD2}$ (Figure 5c,d show the AT1-induced VCB-$Brd4^{BD2}$ and VCB-$Brd4^{BD1}$ complex formation, respectively), with AT1 being more selective than MZ1, in line with published data.[88] Optimal binding was reached when the E3 ligase:PROTAC:POI molar ratio was 1:2:1 (5 μM:10 μM:5 μM), whereas a 20 μM PROTAC concentration led to the so-called 'Hook effect', comprising a decrease in ternary complex formation in the presence of high PROTAC concentrations, which promote binary interactions. Moreover, by comparing the ternary complex formation with a highly cooperative POI ($Brd4^{BD2}$, $\alpha = 4.7$) and a less cooperative one ($Brd4^{BD1}$, $\alpha = 0.2$), nMS experiments captured cooperative PROTAC binding (i.e., binding of the PROTAC to the first protein complex enhances the affinity for the second one, thereby facilitating ternary complex formation over the binary ones; compare Figure 5c and d). Specifically, when AT1 (10 μM) was mixed with 5 μM VCB, the ternary complex fraction was 0.2, whereas it was ~0.5 for both $Brd4^{BD2}$ and $Brd4^{BD1}$ at the same concentrations. Notably, when the three components were incubated together at a ligase:PROTAC:POI 1:2:1 molar ratio, the ternary complex was observed to a much higher extent with $Brd4^{BD2}$ (0.82) than with $Brd4^{BD1}$ (0.65), thus confirming what had previously been observed in other experiments (Figure 5c,d).[88] Finally, competition experiments in the presence of three ($Brd3^{BD2}$, $Brd4^{BD1}$, and $Brd4^{BD2}$) or five ($Brd3^{BD2}$, $Brd4^{BD1}$, $Brd4^{BD2}$, $Brd2^{BD2}$, and BrdT) BET family members simultaneously, confirmed both the preferential binding of AT1 and MZ1 toward $Brd4^{BD2}$ and the higher selectivity of AT1.[87]

More recently, Sternicki and colleagues used nMS to assess the complex formation between VCB and either $Brd4^{BD1}$ or $Brd4^{BD2}$ induced by GNE-987,[89] a recently developed VHL-recruiting Brd4-targeting PROTAC.[90,91] The authors showed that GNE-987 targets $Brd4^{BD1}$ preferentially, with a complex ratio of 0.70 when GNE-987 (7.81 μM) was mixed with equimolar amounts of VCB and $Brd4^{BD1}$ (9 μM). At the same concentrations, the complex ratio for $Brd4^{BD2}$ was 0.34, with maxima reached when GNE-987 was increased up to 15.625 and 31.25 μM (0.44 and 0.45, respectively). Conversely, when GNE-987 was tested at these concentrations in the presence of $Brd4^{BD1}$, the 'hook effect' was apparent, and the ternary complex ratio decreased to ~0.55.[89] These data are in accordance with SPR measurements, which indicate a much higher ternary complex half-life ($t_{1/2}$) for $Brd4^{BD1}$, although the magnitude of the difference between the amount of ternary complex formed for $Brd4^{BD1}$ compared with $Brd4^{BD2}$ as measured by nMS is not as large as the window of difference in SPR $t_{1/2}$ measurements, in which $Brd4^{BD1}$ $t_{1/2}$ is 100-fold longer than that of $Brd4^{BD2}$.[91] Nevertheless, nMS provided a steady-state equilibrium measurement, whereas SPR measured a real-time kinetic event; thus, each measurement is unique and influenced by different factors.

A subsequent study by Song and colleagues described nMS experiments on the VCB–MZ1–$Brd4^{BD2}$ complex on a Fourier-transform ion cyclotron resonance (FT-ICR) mass spectrometer and demonstrated that the VCB–MZ1–$Brd4^{BD2}$ ternary complex dissociates following application of increasing CID voltages, which cause ejection of MZ1, whereas the VCB–$Brd4^{BD2}$ complex, not observed in solution in the absence of MZ1, is retained. Further increases in CID voltages induced the release of the peripheral subunit $Brd4^{BD2}$.[92] IM-MS experiments performed on a quadrupole/ion mobility separation/time-of-flight (Q-IMS-ToF) instrument suggested that the 13+ and 12+ charge states observed in the initial experiments assume a more compact conformation, compared with the 15+ charge state, which exists as an extended conformer, whereas the 14+ charge state is a mixture of the two. In line with this, the application of increasing collision voltages caused the preferential dissociation of MZ1 from the more compact conformers and the preferential ejection of $BRD4^{BD2}$ from the more extended ones. These data demonstrate that higher charge states are characterized by greater Coulombic repulsions and PPIs, whereas the low charge states assume a native-like conformation. To this end, the evidence that VCB and $Brd4^{BD2}$ maintain their interactions even after MZ1 ejection supports the presence of specific intermolecular interactions between VCB and $Brd4^{BD2}$, as described in the corresponding crystal structure.[88] The specific non-covalent interac-

tions between the two proteins during the CID experiments might vary from those found in the gas phase. Therefore, although these studies provide a valuable starting point, they need to be validated with orthogonal experiments. Nonetheless, these three studies demonstrate that PROTAC efficacy can be successfully probed via nMS, and the integration of different approaches and instruments could provide insights into both binding affinities and structural features.

Concluding remarks

The progress that has been achieved in the technology of mass spectrometers has paved the way for nMS to evolve into a remarkably flexible tool for analyzing protein–protein and protein–small molecule interactions. Its great sensitivity, ease of use, speed, broad dynamic range, and minimal sample consumption make it an essential component of the biophysical toolbox widely used for early drug screening campaigns. As the numbers of research groups and studies using nMS for drug discovery applications expand and, consequently, more researchers are trained in this area, the investigation of protein–ligand interactions by nMS will become increasingly regular in drug discovery. nMS will become progressively integrated with other methods, such as ITC, SPR, and structural techniques, such as X-ray crystallography and cryo-EM, offering unparalleled insights into protein–ligand binding and PPI modulation, which will have a substantial influence on future drug development processes.

The increased use of nMS in drug discovery should take place with an understanding of the underlying origins of possible experimental false negatives (gas-phase breakdown of hydrophobic interactions) and false positives (nonspecific binding). To this end, future developments in sample preparation, ionization techniques, and equipment should help to successfully overcome these limitations. Nonetheless, nMS analysis is unique in capturing the effects that ligand binding has in solution, such as impacts on protein complex formation,[85] oligomerization,[69] or enzyme–substrate/co-substrate binding.[70] Moreover, by either monitoring direct ligand binding or the effect of protein–ligand interactions, nMS-based competitive-binding assays can also easily define the specificity of a potential drug for a given binding site. Furthermore, binding sites can be distinguished using the right experimental parameters, showing complicated allosteric processes.[70,76,85,93] In addition, the use of nonvolatile buffers or salts, buffer additives such as charge-reducing agents, and the development of innovative detergents and membrane mimetics in the case of membrane proteins, should help to preserve labile native-like protein–small molecule complexes for nMS detection. In line with this, recent studies demonstrated the feasibility of analyzing both soluble and membrane proteins directly from cell lysates,[67,94] or membrane vesicles,[95,96] respectively, thus preventing potential artifacts that might arise from sample preparation. Given that processing the complex spectra generated by these techniques remains time-consuming and difficult to interpret, advances in data analysis are crucial in this context for enabling the full development of nMS analysis of cell lysates and membrane vesicles. To this end, initial steps have been taken toward the development of software for analyzing intricate mass spectra.[97,98] The integration of currently available software platforms with machine learning and artificial intelligence approaches will accelerate nMS spectral interpretation and allow the pharmaceutical sector to adopt nMS as a standard technique.

Given its great potential in capturing PPIs, we anticipate that nMS will have an ever-increasing role in assessing the potency and mode of action of small molecules functioning as PPI modulators, including PROTACs. In some circumstances, measuring the interaction between two (or more) proteins remains difficult and requires the presence of specific tags or immobilization. By contrast, nMS permits the direct observation of these interactions, quantification of complex formation, analysis of cooperative binding, and accurate assessment of the stoichiometry of multiprotein complexes or oligomers. Therefore, a single experiment yields a plethora of information on the influence of a small molecule on the stability of protein complexes. As seen in the case studies included herein, several groups are already using nMS for the evaluation of PPI modulators, and we anticipate that the pharmaceutical industry will adopt nMS for these applications. To this end, chip-based automated nESI platforms, such as the previously mentioned NanoMate,[53] are pivotal for increasing the throughput of nMS experiments and enabling its application to small-molecule libraries.

Authors' contributions

All authors contributed to this article.

Declaration of interests

The authors declare that the research was conducted in the absence of any commercial or financial relationships that could be construed as a potential conflict of interest.

Data availability

No data was used for the research described in the article.

Acknowledgments

This work was supported by Italian Ministry of University FISR2019_00374 MeDyCa (A.M.), 'Sapienza' Ateneo Project 2021 n. RM12117A61C811CE (D.R.), Regione Lazio Progetti di Gruppi di Ricerca 2020 – A0375-2020-36597 (D.R.). F.F. is supported by the EU's Horizon Europe program under the Marie Skłodowska-Curie grant agreement EpiPolyPharma 101062363.

References

1. Eisenberg D, Marcotte EM, Xenarios I, Yeates TO. Protein function in the post-genomic era. *Nature*. 2000;405:823–826.
2. Yamauchi O. Noncovalent interactions in biocomplexes. *Phys Sci Rev*. 2016;1:20160001.
3. Zhou P, Huang J, Tian F. Specific noncovalent interactions at protein-ligand interface: implications for rational drug design. *Curr Med Chem*. 2012;19:226–238.
4. Su H, Xu Y. Application of ITC-based characterization of thermodynamic and kinetic association of ligands with proteins in drug design. Mini Review. *Front Pharmacol*. 2018;9:1133.
5. O'Connell N. Protein ligand interactions using surface plasmon resonance. *Methods Mol Biol*. 2021;2365:3–20.

6. Becker W, Bhattiprolu KC, Gubensäk N, Zangger K. Investigating protein–ligand interactions by solution nuclear magnetic resonance spectroscopy. *ChemPhysChem*. 2018;19:895–906.
7. Turnbull AP, Emsley P. Studying protein-ligand interactions using X-ray crystallography. *Methods Mol Biol*. 2013;1008:457–477.
8. Benesch JL, Ruotolo BT, Simmons DA, Robinson CV. Protein complexes in the gas phase: technology for structural genomics and proteomics. *Chem Rev*. 2007;107:3544–3567.
9. Liko I, Allison TM, Hopper JT, Robinson CV. Mass spectrometry guided structural biology. *Curr Opin Struct Biol*. 2016;40:136–144.
10. Laganowsky A, Reading E, Hopper JT, Robinson CV. Mass spectrometry of intact membrane protein complexes. *Nat Protoc*. 2013;8:639.
11. Mehmood S, Allison TM, Robinson CV. Mass spectrometry of protein complexes: from origins to applications. *Annu Rev Phys Chem*. 2015;66:453–474.
12. Boeri Erba E, Signor L, Petosa C. Exploring the structure and dynamics of macromolecular complexes by native mass spectrometry. *J Proteomics*. 2020;222 103799.
13. Wilm M, Mann M. Analytical properties of the nanoelectrospray ion source. *Anal Chem*. 1996;68:1–8.
14. Katta V, Chait BT. Observation of the heme-globin complex in native myoglobin by electrospray–ionization mass spectrometry. *J Am Chem Soc*. 1991;113:8534.
15. Ganem B, Li YT, Henion JD. Detection of noncovalent receptor–ligand complexes by mass spectrometry. *J Am Chem Soc*. 1991;113:6294.
16. Kitova EN, El-Hawiet A, Schnier PD, Klassen JS. Reliable determinations of protein-ligand interactions by direct ESI-MS measurements. Are we there yet? *J Am Soc Mass Spectrom*. 2012;23:431–441.
17. Wang W, Kitova EN, Klassen JS. Influence of solution and gas phase processes on protein–carbohydrate binding affinities determined by nanoelectrospray Fourier transform ion cyclotron resonance mass spectrometry. *Anal Chem*. 2003;75:4945.
18. El-Hawiet A, Shoemaker GK, Daneshfar R, Kitova EN, Klassen JS. Applications of a catch and release electrospray ionization mass spectrometry assay for carbohydrate library screening. *Anal Chem*. 2012;84:50–58.
19. Sun J, Kitova EN, Klassen JS. Method for stabilizing protein−ligand complexes in nanoelectrospray ionization mass spectrometry. *Anal Chem*. 2007;79:416–425.
20. Allison TM, Bechara C. Structural mass spectrometry comes of age: new insight into protein structure, function and interactions. *Biochem Soc Trans*. 2019;47:317–327.
21. Fiorentino F, Bolla JR. Mass spectrometry analysis of dynamics and interactions of the LPS translocon LptDE. *Methods Mol Biol*. 2022;2548:109–128.
22. McDowell MA et al.. Structural basis of tail-anchored membrane protein biogenesis by the GET insertase complex. *Mol Cell*. 2020;80:72–86.
23. Olinares PDB et al.. Native mass spectrometry-based screening for optimal sample preparation in single-particle cryo-EM. *Structure*. 2021;29:186.
24. Agasid MT, Sørensen L, Urner LH, Yan J, Robinson CV. The effects of sodium ions on ligand binding and conformational states of G protein-coupled receptors—insights from mass spectrometry. *J Am Chem Soc*. 2021;143:4085–4089.
25. Nguyen GTH, Tran TN, Podgorski MN, Bell SG, Supuran CT, Donald WA. Nanoscale ion emitters in native mass spectrometry for measuring ligand-protein binding affinities. *ACS Cent Sci*. 2019;5:308–318.
26. Townsend JA, Keener JE, Miller ZM, Prell JS, Marty MT. Imidazole derivatives improve charge reduction and stabilization for native mass spectrometry. *Anal Chem*. 2019;91:14765–14772.
27. Shimon L, Sharon M, Horovitz A. A method for removing effects of nonspecific binding on the distribution of binding stoichiometries: application to mass spectroscopy data. *Biophys J*. 2010;99:1645–1649.
28. Gault J et al.. Combining native and 'omics' mass spectrometry to identify endogenous ligands bound to membrane proteins. *Nat Methods*. 2020;17:505–508.
29. Gault J et al.. High-resolution mass spectrometry of small molecules bound to membrane proteins. *Nat Methods*. 2016;13:333–336.
30. Sobott F, Hernández H, McCammon MG, Tito MA, Robinson CV. A tandem mass spectrometer for improved transmission and analysis of large macromolecular assemblies. *Anal Chem*. 2002;74:1402.
31. Laganowsky A et al.. Membrane proteins bind lipids selectively to modulate their structure and function. *Nature*. 2014;510:172–175.
32. Xie Y, Zhang J, Yin S, Loo JA. Top-down ESI-ECD-FT-ICR mass spectrometry localizes noncovalent protein-ligand binding sites. *J Am Chem Soc*. 2006;128:14432.
33. Li H, Nguyen HH, Ogorzalek Loo RR, Campuzano IDG, Loo JA. An integrated native mass spectrometry and top-down proteomics method that connects sequence to structure and function of macromolecular complexes. *Nat Chem*. 2018;10:139–148.
34. Barrera NP, Di Bartolo N, Booth PJ, Robinson CV. Micelles protect membrane complexes from solution to vacuum. *Science*. 2008;321:243–246.
35. Urner LH et al.. Anionic dendritic polyglycerol for protein purification and delipidation. *ACS Appl Polym Mater*. 2021;3:5903–5911.
36. Bolla JR, Agasid MT, Mehmood S, Robinson CV. Membrane protein-lipid interactions probed using mass spectrometry. *Annu Rev Biochem*. 2019;88:85–111.
37. Bolla JR, Fiorentino F, Robinson CV. Mass spectrometry informs the structure and dynamics of membrane proteins involved in lipid and drug transport. *Curr Opin Struct Biol*. 2021;70:53–60.
38. Fiorentino F et al.. Dynamics of an LPS translocon induced by substrate and an antimicrobial peptide. *Nat Chem Biol*. 2021;17:187–195.
39. Fiorentino F, Mai A, Rotili D. Lysine acetyltransferase inhibitors: structure–activity relationships and potential therapeutic implications. *Future Med Chem*. 2018;10:1067–1091.
40. Yen HY et al.. Ligand binding to a G protein-coupled receptor captured in a mass spectrometer. *Sci Adv*. 2017;3:e1701016.
41. Yen HY et al.. PtdIns(4,5)P2 stabilizes active states of GPCRs and enhances selectivity of G-protein coupling. *Nature*. 2018;559:423–427.
42. Urner LH et al.. Modular detergents tailor the purification and structural analysis of membrane proteins including G-protein coupled receptors. *Nat Commun*. 2020;11:564.
43. Laganowsky A, Clemmer DE, Russell DH. Variable-temperature native mass spectrometry for studies of protein folding, stabilities, assembly, and molecular interactions. *Annu Rev Biophys*. 2022;51:63–77.
44. Marcoux J et al.. Mass spectrometry reveals synergistic effects of nucleotides, lipids, and drugs binding to a multidrug resistance efflux pump. *Proc Natl Acad Sci U S A*. 2013;110:9704–9709.
45. Mehmood S et al.. Mass spectrometry captures off-target drug binding and provides mechanistic insights into the human metalloprotease ZMPSTE24. *Nat Chem*. 2016;8:1152–1158.
46. Liko I et al.. Lipid binding attenuates channel closure of the outer membrane protein OmpF. *Proc Natl Acad Sci U S A*. 2018;115:6691–6696.
47. Bolla JR, Sauer JB, Wu D, Mehmood S, Allison TM, Robinson CV. Direct observation of the influence of cardiolipin and antibiotics on lipid II binding to MurJ. *Nat Chem*. 2018;10:363–371.
48. Fiorentino F, Bolla JR, Mehmood S, Robinson CV. The different effects of substrates and nucleotides on the complex formation of ABC transporters. *Structure*. 2019;27:651–659.
49. Bennett JL, Nguyen GTH, Donald WA. Protein-small molecule interactions in native mass spectrometry. *Chem Rev*. 2022;122:7327–7385.
50. Gavriilidou AFM, Sokratous K, Yen HY, De Colibus L. High-throughput native mass spectrometry screening in drug discovery. *Front Mol Biosci*. 2022;9 837901.
51. Vu H et al.. Fragment-based screening of a natural product library against 62 potential malaria drug targets employing native mass spectrometry. *ACS Infect Dis*. 2018;4:431–444.
52. Nguyen GTH et al.. Multiplexed screening of thousands of natural products for protein-ligand binding in native mass spectrometry. *J Am Chem Soc*. 2021;143:21379–21387.
53. Zhang S, Van Pelt CK, Wilson DB. Quantitative determination of noncovalent binding interactions using automated nanoelectrospray mass spectrometry. *Anal Chem*. 2003;75:3010–3018.
54. Supuran CT. Carbonic anhydrases: novel therapeutic applications for inhibitors and activators. *Nat Rev Drug Discov*. 2008;7:168–181.
55. Alterio V, Di Fiore A, D'Ambrosio K, Supuran CT, De Simone G. Multiple binding modes of inhibitors to carbonic anhydrases: how to design specific drugs targeting 15 different isoforms? *Chem Rev*. 2012;112:4421–4468.
56. Park H, Jung J, Rodrigues E, Kitova EN, Macauley MS, Klassen JS. Mass spectrometry-based shotgun glycomics for discovery of natural ligands of glycan-binding proteins. *Anal Chem*. 2020;92:14012–14020.
57. White KL et al.. Structural connection between activation microswitch and allosteric sodium site in GPCR signaling. *Structure*. 2018;26:259–269.
58. Ren C et al.. Quantitative determination of protein-ligand affinity by size exclusion chromatography directly coupled to high-resolution native mass spectrometry. *Anal Chem*. 2019;91:903–911.
59. Cheng C et al.. Identifying new ligands for JNK3 by fluorescence thermal shift assays and native mass spectrometry. *ACS Omega*. 2022;7:13925–13931.
60. D'Amico CI, Polasky DA, Steyer DJ, Ruotolo BT, Kennedy RT. Ion mobility-mass spectrometry coupled to droplet microfluidics for rapid protein structure analysis and drug discovery. *Anal Chem*. 2022;94:13084–13091.

61. Benesch JL, Ruotolo BT. Mass spectrometry: come of age for structural and dynamical biology. *Curr Opin Struct Biol*. 2011;21:641–649.
62. Fiorentino F, Castiello C, Mai A, Rotili D. Therapeutic potential and activity modulation of the protein lysine deacylase sirtuin 5. *J Med Chem*. 2022;65:9580–9606.
63. Fiorentino F, Mautone N, Menna M, D'Acunzo F, Mai A, Rotili D. Sirtuin modulators: past, present, and future perspectives. *Future Med Chem*. 2022;14:915–939.
64. Taurone S et al.. Biochemical functions and clinical characterizations of the sirtuins in diabetes-induced retinal pathologies. *Int J Mol Sci*. 2022;23:4048.
65. Dixit SM, Polasky DA, Ruotolo BT. Collision induced unfolding of isolated proteins in the gas phase: past, present, and future. *Curr Opin Chem Biol*. 2018;42:93–100.
66. Kaur H et al.. The antibiotic darobactin mimics a beta-strand to inhibit outer membrane insertase. *Nature*. 2021;593:125–129.
67. Rogawski R et al.. Intracellular protein-drug interactions probed by direct mass spectrometry of cell lysates. *Angew Chem Int Ed Engl*. 2021;60:19637–19642.
68. Olinares PDB, Dunn AD, Padovan JC, Fernandez-Martinez J, Rout MP, Chait BT. A robust workflow for native mass spectrometric analysis of affinity-isolated endogenous protein assemblies. *Anal Chem*. 2016;88:2799–2807.
69. Fiorentino F, Rotili D, Mai A, Bolla JR, Robinson CV. Mass spectrometry enables the discovery of inhibitors of an LPS transport assembly via disruption of protein–protein interactions. *Chem Commun (Camb)*. 2021;57:10747–10750.
70. El-Baba TJ et al.. Allosteric inhibition of the SARS-CoV-2 main protease: insights from mass spectrometry based assays. *Angew Chem Int Ed Engl*. 2020;59:23544–23548.
71. Bolla JR, Howes AC, Fiorentino F, Robinson CV. Assembly and regulation of the chlorhexidine-specific efflux pump AceI. *Proc Natl Acad Sci U S A*. 2020;117:17011–17018.
72. Lundstedt E, Kahne D, Ruiz N. Assembly and maintenance of lipids at the bacterial outer membrane. *Chem Rev*. 2020;121:5098–5123.
73. Bollati M et al.. Crystal structure of LptH, the periplasmic component of the lipopolysaccharide transport machinery from *Pseudomonas aeruginosa*. *FEBS J*. 2015;282:1980–1997.
74. Douangamath A et al.. Crystallographic and electrophilic fragment screening of the SARS-CoV-2 main protease. *Nat Commun*. 2020;11:5047.
75. Zhu D et al.. Efficient discovery of potential inhibitors for SARS-CoV-2 3C-like protease from herbal extracts using a native MS-based affinity-selection method. *J Pharm Biomed Anal*. 2022;209 114538.
76. Moghadamchargari Z et al.. Molecular assemblies of the catalytic domain of SOS with KRas and oncogenic mutants. *Proc Natl Acad Sci U S A*. 2021;118. e2022403118.
77. Janes MR et al.. Targeting KRAS mutant cancers with a covalent G12C-specific inhibitor. *Cell*. 2018;172:578–589.
78. Shima F et al.. In silico discovery of small-molecule Ras inhibitors that display antitumor activity by blocking the Ras-effector interaction. *Proc Natl Acad Sci U S A*. 2013;110:8182–8187.
79. Hillig RC et al.. Discovery of potent SOS1 inhibitors that block RAS activation via disruption of the RAS-SOS1 interaction. *Proc Natl Acad Sci U S A*. 2019;116:2551–2560.
80. Hofmann MH et al.. BI-3406, a potent and selective SOS1-KRAS interaction inhibitor, is effective in KRAS-driven cancers through combined MEK inhibition. *Cancer Discov*. 2021;11:142–157.
81. Bellamy-Carter J et al.. Discovering protein-protein interaction stabilisers by native mass spectrometry. *Chem Sci*. 2021;12:10724–10731.
82. De Vries-van Leeuwen IJ et al.. Interaction of 14-3-3 proteins with the Estrogen Receptor Alpha F domain provides a drug target interface. *Proc Natl Acad Sci U S A*. 2013;110:8894–8899.
83. Stevers LM, De Vries RMJM, Doveston RG, Milroy LG, Brunsveld L, Ottmann C. Structural interface between LRRK2 and 14-3-3 protein. *Biochem J*. 2017;474:1273–1287.
84. Doveston RG et al.. Small-molecule stabilization of the p53–14-3-3 protein-protein interaction. *FEBS Lett*. 2017;591:2449–2457.
85. Yen HY et al.. Mass spectrometry captures biased signalling and allosteric modulation of a G-protein-coupled receptor. *Nat Chem*. 2022;14:1375–1382.
86. Tomaselli D, Mautone N, Mai A, Rotili D. Recent advances in epigenetic proteolysis targeting chimeras (epi-PROTACs). *Eur J Med Chem*. 2020;207 112750.
87. Beveridge R, Kessler D, Rumpel K, Ettmayer P, Meinhart A, Clausen T. Native mass spectrometry can effectively predict PROTAC efficacy. *ACS Cent Sci*. 2020;6:1223–1230.
88. Gadd MS et al.. Structural basis of PROTAC cooperative recognition for selective protein degradation. *Nat Chem Biol*. 2017;13:514–521.
89. Sternicki LM, Nonomiya J, Liu M, Mulvihill MM, Quinn RJ. Native mass spectrometry for the study of PROTAC GNE-987-containing ternary complexes. *ChemMedChem*. 2021;16:2206–2210.
90. Fidanze SD et al.. Discovery and optimization of novel constrained pyrrolopyridone BET family inhibitors. *Bioorg Med Chem Lett*. 2018;28:1804–1810.
91. Pillow TH et al.. Antibody conjugation of a chimeric BET degrader enables *in vivo* activity. *ChemMedChem*. 2020;15:17–25.
92. Song JH et al.. Native mass spectrometry and gas-phase fragmentation provide rapid and in-depth topological characterization of a PROTAC ternary complex. *Cell Chem Biol*. 2021;28:1528–1538.
93. Patrick JW et al.. Allostery revealed within lipid binding events to membrane proteins. *Proc Natl Acad Sci U S A*. 2018;115:2976–2981.
94. Vimer S, Ben-Nissan G, Sharon M. Mass spectrometry analysis of intact proteins from crude samples. *Anal Chem*. 2020;92:12741.
95. Chorev DS et al.. Protein assemblies ejected directly from native membranes yield complexes for mass spectrometry. *Science*. 2018;362:829.
96. Chen S et al.. Capturing a rhodopsin receptor signalling cascade across a native membrane. *Nature*. 2022;604:384–390.
97. Quetschlich D et al.. NaViA: a program for the visual analysis of complex mass spectra. *Bioinformatics*. 2021;37:4876–4878.
98. Marty MT, Baldwin AJ, Marklund EG, Hochberg GK, Benesch JL, Robinson CV. Bayesian deconvolution of mass and ion mobility spectra: from binary interactions to polydisperse ensembles. *Anal Chem*. 2015;87:4370–4376.